

Digital Characterization of Particle Tracks for Microdosimetry¹

J. E. Turner, R. N. Hamm, G. S. Hurst, H. A. Wright

Health and Safety Research Division

and

CONF-850506--6

M. M. Chiles

DE85 012898

Instrumentation and Controls Division
Oak Ridge National Laboratory
Oak Ridge, Tennessee

Digital Characterization...Tracks

DISCLAIMER

This report was prepared as an account of work sponsored by an agency of the United States Government. Neither the United States Government nor any agency thereof, nor any of their employees, makes any warranty, express or implied, or assumes any legal liability or responsibility for the accuracy, completeness, or usefulness of any information, apparatus, product, or process disclosed, or represents that its use would not infringe privately owned rights. Reference herein to any specific commercial product, process, or service by trade name, trademark, manufacturer, or otherwise does not necessarily constitute or imply its endorsement, recommendation, or favoring by the United States Government or any agency thereof. The views and opinions of authors expressed herein do not necessarily state or reflect those of the United States Government or any agency thereof.

By acceptance of this article, the publisher or recipient acknowledges the U.S. Government's right to retain a nonexclusive, royalty-free license in and to any copyright covering the article.

DISTRIBUTION OF THIS DOCUMENT IS UNLIMITED

je

FOOTNOTES

¹Research sponsored by the Office of Health and Environmental Research, U.S. Department of Energy, under contract DE-AC05-84OR21400 with Martin Marietta Energy Systems, Inc.

Digital Characterization of Particle Tracks for Microdosimetry

J. E. Turner, R. N. Hamm, G. S. Hurst, H. A. Wright, and M. M. Chiles

ABSTRACT

Work is in progress to develop a digital approach to microdosimetry and to construct a prototype instrument to obtain digital information about charged-particle tracks. The objective of such a device is to measure the numbers of electrons produced in various subvolumes of a chamber gas along a particle's path. This paper describes results of Monte Carlo calculations of charged-particle tracks in a cubical time-projection ionization chamber containing methane. Results are presented to show the effects of electron diffusion during charge collection. The calculations indicate that the optimum ratio of field strength and pressure is about $0.6 \text{ volts cm}^{-1} \text{ torr}^{-1}$. Examples of proton, carbon-ion, and electron tracks are shown.

INTRODUCTION

Measurement of the numbers of ion pairs in various volume elements along a charged particle's path in a gas would provide digital information about the track. Knowledge of the original position coordinates of every electron collected in an ionization chamber would represent a complete description of the ionization track. The present work presents some calculations for a time-projection chamber in the shape of a cube, having edges 10 cm in length. The electrons produced in the chamber drift parallel to the Z axis under the influence of an applied field and are collected on the XY plane. To within the resolution of the detection system, the coordinates (x, y) of their arrival in the collecting plane is measured by an array of detectors in that plane; the drift distance z of the electrons is obtained from the measured time of arrival in the collecting plane.

This is the second report on this work. The first paper⁽¹⁾ presented some calculations for protons in a chamber containing P-10 gas (90% Ar and 10% CH₄). The present paper gives results of calculations made for protons, carbon ions, and electrons in methane. The effect of electron diffusion during collection is studied. Several examples show how different chamber specifications could be used, depending on the particular application for the chamber, i.e., dosimetry, LET measurements, or measurement of microdosimetric distributions.

CALCULATIONAL APPROACH

As described in more detail in Ref. (1), we have developed a Monte Carlo computer code to calculate the detailed transport of heavy charged particles and electrons in mixtures of argon and methane. The code can transport all particles until their energies go below the threshold for

producing ionization in the gas. For a charged particle in the chamber, we thus calculate the positions of all of the electrons as they reach subexcitation energies. These are the electrons collected, either under saturation conditions or with gas multiplication, to produce a signal in response to the interaction of the charged particle with the gas.

To perform the Monte Carlo calculations, sets of cross sections have been constructed for ionization and excitation of methane and argon molecules by protons and carbon ions as functions of particle energy. For electrons, we have used a modified version of a Monte Carlo code we developed for water. As described earlier,⁽¹⁾ experimental cross-section data are used insofar as they are available for choosing flight distances and energy losses. Otherwise, "phenomenological" cross sections are used, which we selected to be consistent with stopping powers and W values at energies for which such information is available. Our stopping ions thus produce the "right" amount of ionization in the gases, consistent with experimental data.

DIFFUSION

The calculations simulate the diffusion of electrons as determined by measured values of D/μ (the ratio of the diffusion coefficient D and mobility μ) as a function of E/P (the ratio of the electric field strength E and the pressure P of the gas in the chamber). The data of Hunter, Carter, Christophorou, and Lakdawala⁽²⁾ for CH_4 were used in the present calculations. The projection of the root-mean-square diffusion distance in any direction during a drift time t is given by $\lambda = \sqrt{2Dt}$. If the drift distance is z and the drift velocity is w , then $t = z/w$. In terms of the electron mobility, $w = \mu E$; therefore

$$\lambda = \sqrt{\frac{2z}{E} \cdot \frac{D}{\mu}} \quad (1)$$

As a measure of the relative effect of electron diffusion, one can use the value λ_1 calculated for $z = 1$ cm: $\lambda_1 = \sqrt{(2/E)} (D/\mu)$. Plots of this quantity as a function of E/P for CH_4 at three values of chamber pressure are shown in Fig. 1. While D/μ depends only on E/P , the value of λ_1 also depends inversely on \sqrt{E} . As seen from the figure, diffusion is minimized in the range $0.4 \lesssim E/P \lesssim 1.0$ in the pressure range from 1-100 torr. The examples below will illustrate how the digital characterization of a track is affected by the pressure.

EXAMPLES OF PROTON, CARBON-ION, AND ELECTRON TRACKS

Figure 2 shows the track of a 500 keV proton, traveling parallel to the Y axis and entering a $10 \times 10 \times 10$ cm³ methane chamber near the center of its XZ face, as indicated by the arrow. For this example, we envision a uniform 10×10 cm² array of detectors in the XY plane, represented by the squares shown there. Each dot in Fig. 2 shows the position of one of the 1605 subexcitation electrons produced in the chamber by this proton, which loses 47.6 keV in traversing it. The field-strength and pressure are $E = 10$ volts/cm and $P = 10$ torr ($E/P = 1.0$ volts cm⁻¹ torr⁻¹).

To simulate the diffusion of the electrons as they drift to the detectors in the XY plane, we displaced the original (x,y,z) coordinates of the electrons in the following manner. From the z coordinate of each electron, we calculated the root-mean-square diffusion distance λ from Eq. (1), above. A computer library program was then used to randomly select displacements in the X, Y, and Z directions from a Gaussian distribution having that value of λ . The displaced positions, which would be those inferred from the arrivals of the diffused electrons in the XY plane with precise resolution, are shown in Fig. 3 for the same

track as in Fig. 2. Tracks nearer the collection plane would appear less spread out, while those further away would be more diffuse. Of the original 1605 electrons produced by the proton in Fig. 1, 45 diffuse out of the chamber (through the walls $y = 0$ and $y = 10$) before reaching the XY plane.

Figure 4 shows the appearance of the track of an 80-keV carbon ion which entered the chamber the same way as the proton. This carbon ion is stopped by ~ 2.2 cm of the chamber gas and produces 1622 electrons, the initial energy being selected to produce about the same number of initial ionizations as the proton in Fig. 2. Figure 4 shows the carbon track after diffusion, as it would "appear" after collection in the XY plane. Only 1405 of the original 1622 electrons are collected, since many diffuse out of the chamber through the XZ plane ($y = 0$). Because of the difference in the W values for the track segment of the 500 keV proton and the stopping carbon ion, energy proportionality exists only to within a factor of ~ 2 , even apart from the relatively larger number of electrons that diffuse out of the chamber from the carbon ion. However, the chamber's ability to discriminate between the spatial patterns of the events in Figs. 3 and 4 is clearly evident.

The track of a 100-keV electron, entering the chamber along the same path as the other ions, is shown in Fig. 5. In order to have more than just a few ionizations, the gas pressure for the electron was increased to 100 torr and the field strength to 100 volts/cm, maintaining $E/P = 1.0$ volts cm^{-1} torr $^{-1}$, as before. The electron lost 2.55 keV of energy and produced 96 ion pairs in traversing the chamber. As seen from Fig. 1, the increased field strength with the same E/P reduces the

root-mean-square diffusion distance by a factor of $\sqrt{10}$. The appearance of the track after diffusion is shown in Fig. 6. In this example, 2 of the original 96 electrons diffused out of the chamber without being collected.

DISCUSSION

This paper summarizes work done to date on studies of the feasibility of designing a time-projection chamber to obtain digital information about charged-particle tracks. The examples presented here illustrate the different spatial patterns of the electrons collected as the result of the passage of a proton, carbon ion, or electron in the chamber gas. The particular design criteria for a prototype chamber would depend on the use for which it is intended. With the particular version presented here, for example, the proton in Fig. 3 would be distinguished from the carbon ion in Fig. 4, even though both produced a comparable amount of ionization. The number of electrons in most volume elements where ionization occurs is large enough to permit proportional counting by the detectors in the XY plane, so that the amount of dose deposited in the gas by the proton or carbon ion could be measured. This measurement, together with the knowledge of the spatial extent of the tracks, would enable LET in the gas to be determined. Such information is directly relevant to neutron dosimetry. For microdosimetry, determination of the energy absorbed in the various volume elements would provide the distributions in specific energy from single events. Whereas the amount of diffusion exemplified by Figs. 2 and 3 would not be critical for neutron dosimetry, it would adversely affect the determination of single-event spectra. A smaller or flatter chamber would be more appropriate for this purpose.

Other combinations of particle LET, gas pressure, and electric field strength can give tracks with an appearance like that in Fig. 6. In this regime, one approaches the "ultimate" digital characterization of a track in which the position of every electron in a track segment is determined. (With sufficient resolution, a track is characterized by binary information; each volume element in the chamber contains with high probability either 0 or 1 subexcitation electron.) In principle, one can thus obtain information about correlations and proximity relationships.

The next phase of this work will be concerned with the development of an analysis algorithm for converting measured responses in the detectors into information about the track that produced them.

REFERENCES

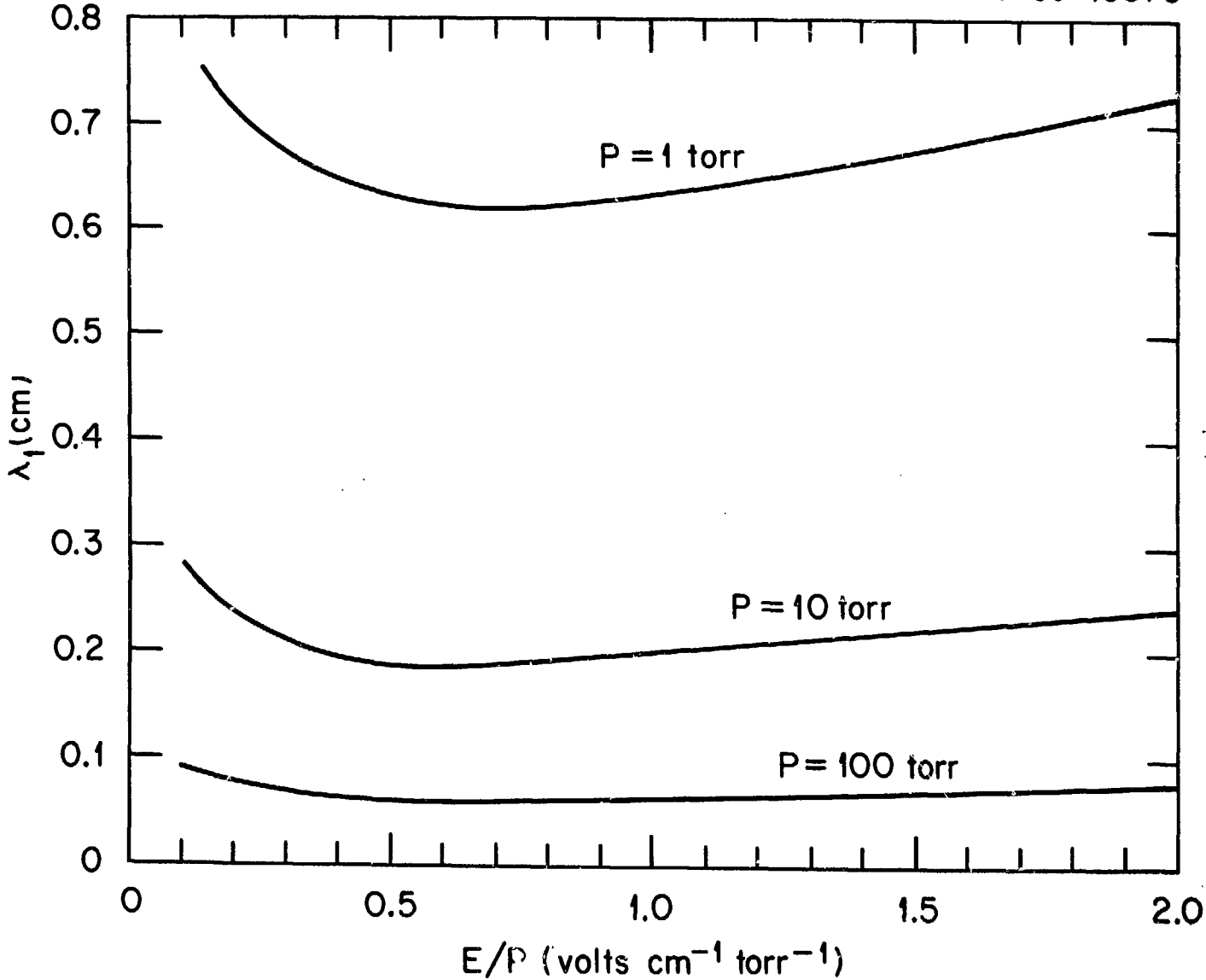
1. Turner, J. E., Hamm, R. N., Hurst, G. S., Wright, H. A., and Chiles, M. M. Studies of a Digital Approach to Neutron Dosimetry and Microdosimetry. In Proceedings of the Fifth Symposium on Neutron Dosimetry, Neuherberg, FRG, September 17-21, 1984. Commission of the European Communities, in press.
2. Hunter, S. R., Carter, J. G., Christophorou, L. G., and Lakdawala, V. K. Transport Properties and Dielectric Strength of Gas Mixtures for Use in Diffuse Discharge Opening Switches. Gaseous Dielectrics IV, Proc. Fourth Int. Symp. on Gaseous Dielectrics, Knoxville, Tennessee, April 29-May 3, 1984, p. 24, L. G. Christophorou and M. O. Pace, eds., Pergamon Press, New York (1984).

FIGURE CAPTIONS

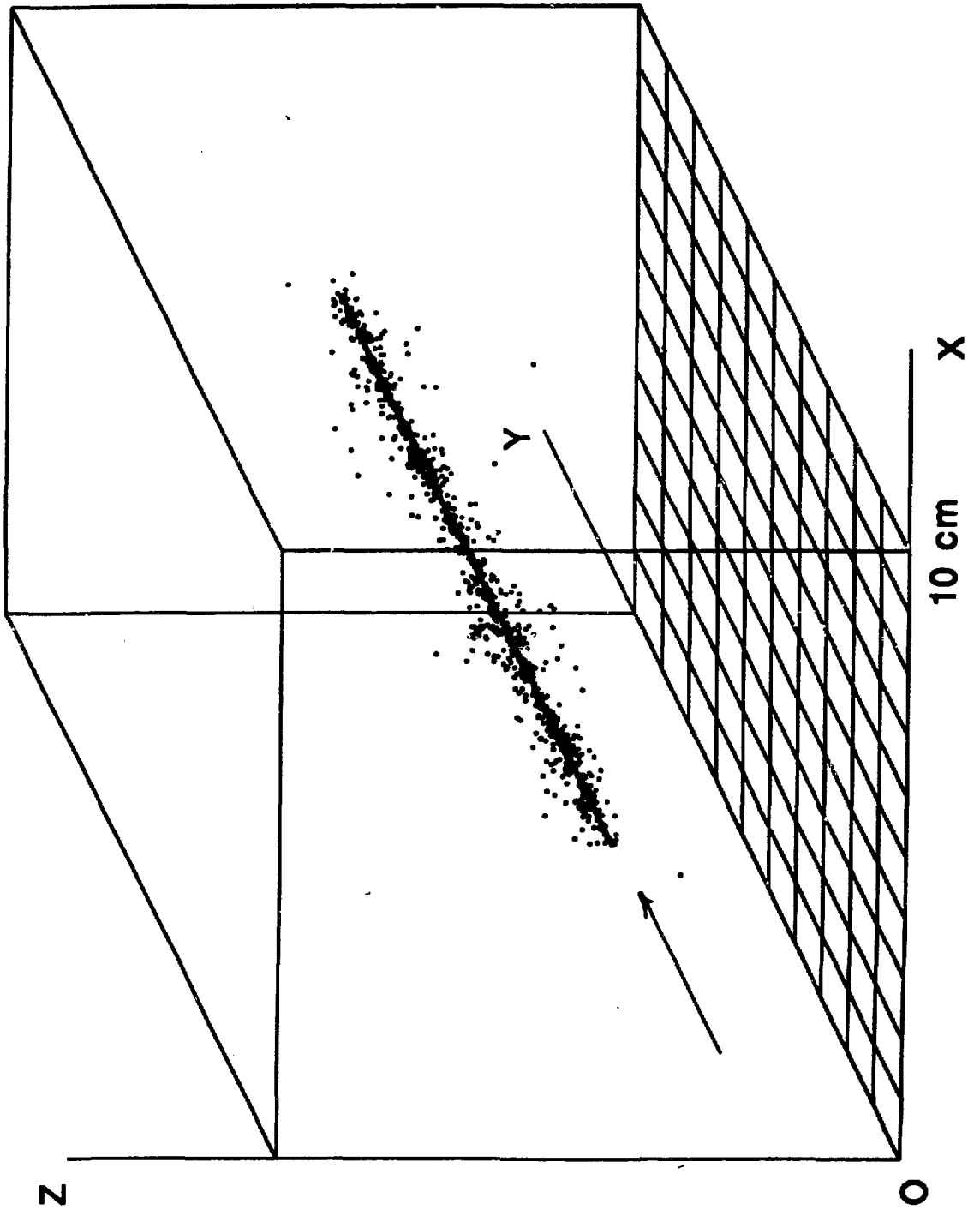
- Fig. 1. Projected root-mean-square electron diffusion distance, λ_1 , for a drift distance of 1 cm as a function of E/P for pressures of 1, 10, and 100 torr.
- Fig. 2. Track of 500 keV proton traversing the CH₄ chamber before electron diffusion, with E = 10 volts/cm and P = 10 torr. The grid in the XY plane represents an array of 100 detectors, each having a sensitive area 1 cm × 1 cm. The chamber gas occupies a cubic volume, having 10 cm edges. This proton deposits 47.6 keV of energy and produces 1605 subexcitation electrons, represented by the dots.
- Fig. 3. Appearance of track in Fig. 2 after diffusion of electrons into the XY collection plane. A total of 1560 of the original 1605 subexcitation electrons reach the XY plane, the others having diffused out through the walls $y = 0$ and $y = 10$ cm.
- Fig. 4. Appearance of the track of an 80 keV carbon ion (after diffusion) entering the chamber in the same way as the proton in the previous figures, with E = 10 volts/cm and P = 10 torr, the same as before. Both the proton and carbon ion produce about the same number of subexcitation electrons originally in the chamber (1605 by the proton and 1622 by the carbon ion).

Fig. 5. Track of 100 keV electron traversing chamber along same path as the proton in the previous figures. In this instance, $P = 100$ torr and $E = 100$ volts/cm. This electron produces 96 ion pairs and loses 2.55 keV of energy in the chamber.

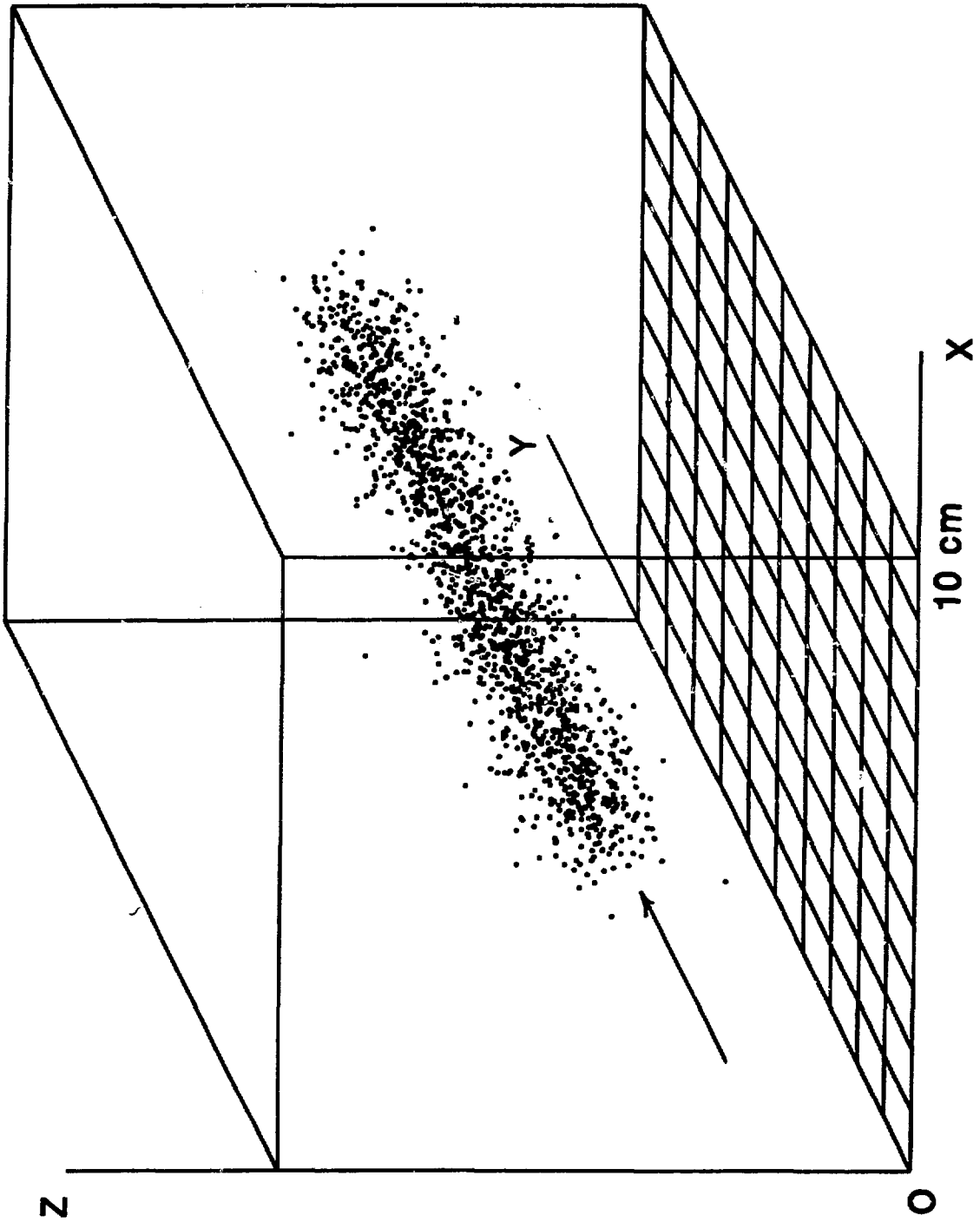
Fig. 6. Electron track from Fig. 5 after diffusion. Two of the original 96 electrons diffuse through the chamber walls ($y = 0$ and $y = 10$ cm) without reaching the detectors in the XY plane.

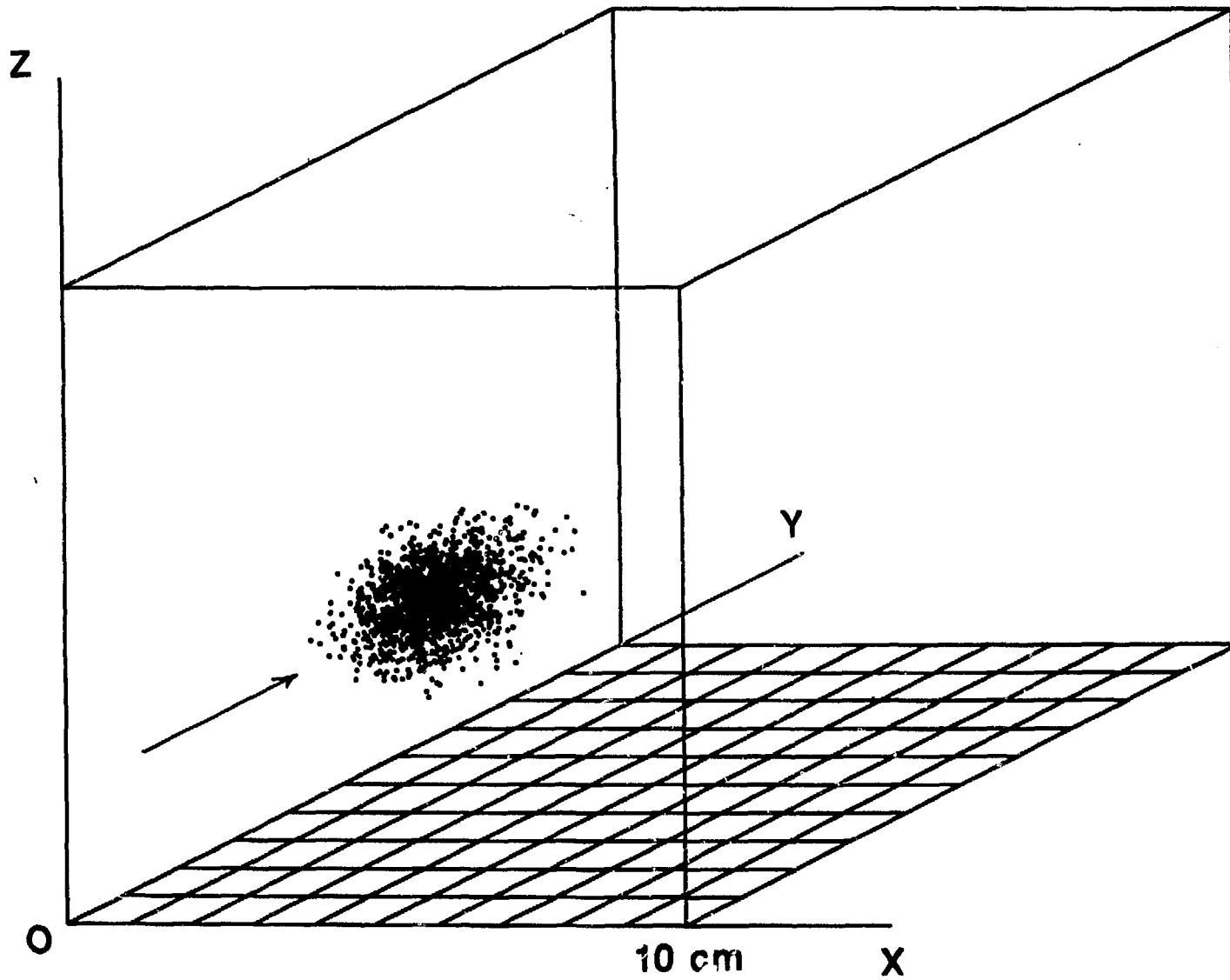


ORNL-DWG 85-10510

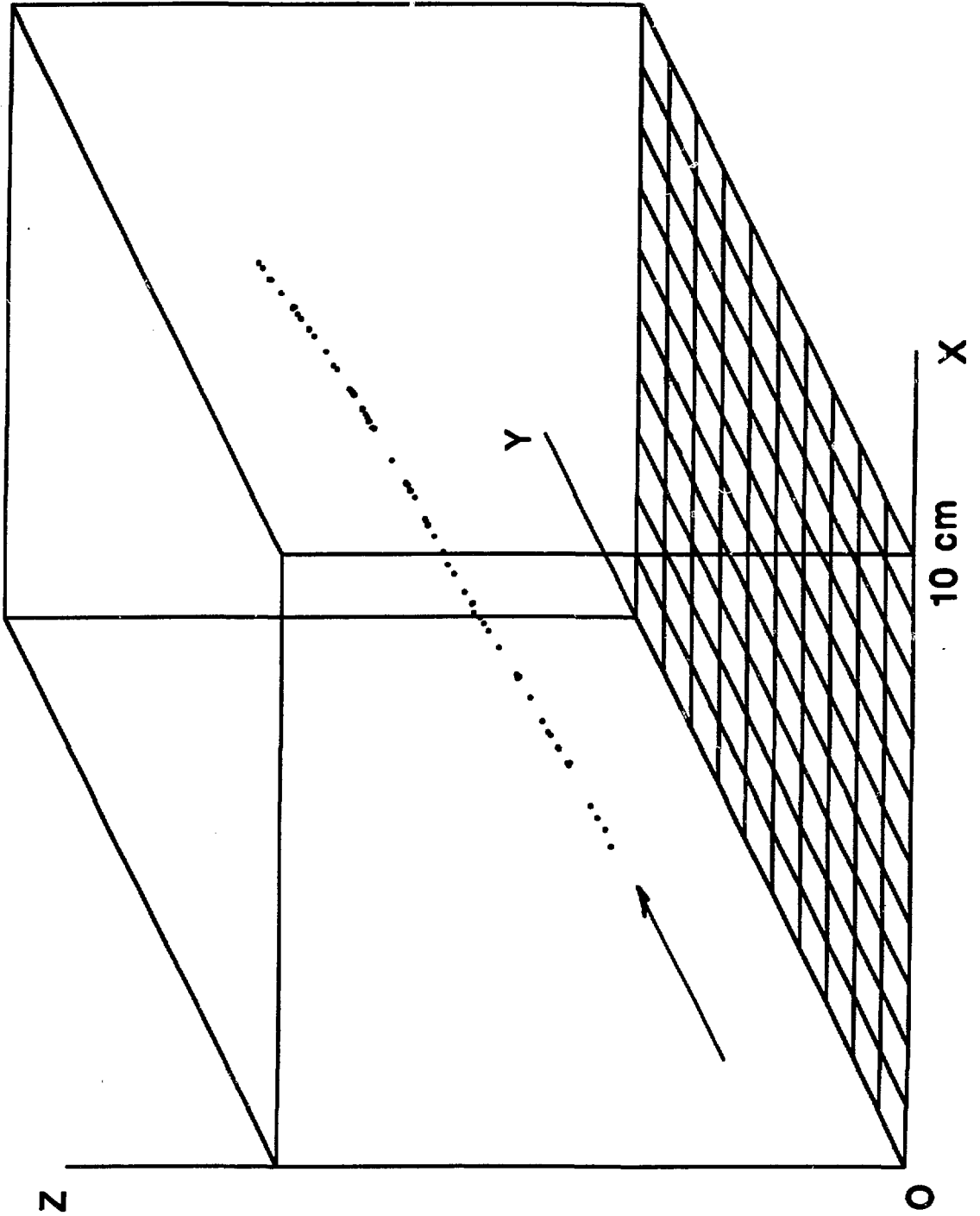


ORNL-DWG 85-10511





ORNL-DWG 85-10513



ORNL-DWG 85-10514

